Carbon-Coated Nanophase $CaMoO_4$ as Anode Material for Li Ion Batteries

N. Sharma,[†] K. M. Shaju,[†] G. V. Subba Rao,[†] B. V. R. Chowdari,*[,†]
Z. L. Dong,[‡] and T. J. White[‡]

Department of Physics, National University of Singapore, Singapore 117542, and Centre for Advanced Research of Ecomaterials, Institute of Environmental Science and Engineering, Nanyang Technological University, Singapore 637723

Received September 8, 2003. Revised Manuscript Received November 20, 2003

Pure and carbon (C)-coated $CaMoO_4$ were synthesized by solution precipitation and sol−gel methods, and their electrochemical properties were studied vs Li by galvanostatic cycling and cyclic voltammetry (CV). Combined X-ray diffraction, SEM, and TEM results revealed the formation of nanocrystalline particles with the scheelite structure, the morphology being a function of the synthetic procedure. TEM of 10% C-coated $CaMoO_4$ shows the amorphous nature of carbon on the crystalline particles with a thickness of 8−12 nm. Galvanostatic data in the voltage range of 0.005−2.5 V up to 50 cycles at a rate of 60 mA/g revealed that the 10% C-coated $CaMoO_4$ gave the highest reversible capacities. At the 20th discharge cycle, the capacity values (mA h/g) are as follows: solution precipitated, 190; sol−gel, 268; 5% C-coated, 401; and 10% C-coated, 508. The latter value corresponds to 3.8 mol of recyclable Li. The improvement in the interparticle electronic conductivity imparted by the C-coating led to superior performance. The Coulombic efficiency for all the compositions is >98%. Galvanostatic cycling results are supplemented by the CV data. A plausible mechanism for charge−discharge cycling has been proposed.

Introduction

Recently, vanadium (V) and moybdenum (Mo) containing mixed oxides have received attention as possible negative electrode (anode) materials to replace the graphite presently being used in the Li-ion batteries (LIB).[1−14] This is due to the ability of the above metal ions to exist in several oxidation states in oxides, ranging from 2+ to 5+ for V and 3+ to 6+ for Mo and reversibly reacting with Li at potentials lower than 2 V. The vanadium compounds $LiNiVO_4$,[3] $Co_2V_2O_7$,[3] $MV_2O_{6+\delta}\cdot nH_2O$ (M = Mn, Co),[4] and MnV_2O_6[5] and compounds containing Mo of the type $Mn_{1-x}(V_{1-x}Mo_x)_2O_6$[6,7] ($x$ = 0 and 0.4) and solid solutions SnO_2–MoO_2[8] have been investigated. Studies by the group of Nazar[9−11] on the compounds MoO_3 and $Na_{0.25}MoO_3$ (Na−Mo bronze) and that of Wakihara[12−14] on $MnMoO_4$ showed that first-charge capacities as high as 800−1000 mA h/g can be obtained when tested as positive electrodes vs Li metal. These values are much higher than the 372 mA h/g obtainable with graphite electrodes (vs Li). Also, the high density of the Mo oxides can give rise to higher volumetric energy density of the electrode as compared to graphite. Further, the countercations (Na or Mn), which do not participate in the electrochemical process with Li in the voltage range of interest, may play some role as "spectator" atoms/ions.[9−14] However, capacity-fading was noticed in $Na_{0.25}MoO_3$ when cycled in the voltage range of 0.005−3.5 V at C/20 rate (45 mA/g).[10,11] Similarly, with $MnMoO_4$ the first-charge capacity decreased by more than 50% after 25 cycles at a current density of 0.2 mA/cm^2 in the voltage range of 0−2.0 V vs Li.[12]

The Na−Mo bronze and MoO_3 mentioned above have Mo in octahedral MoO_6 coordination, whereas $MnMoO_4$ has Mo^{6+} in MoO_4 tetrahedral and Mn^{2+} in heavily distorted MnO_6 octahedral O-coordination. The latter compound adopts a monoclinic structure that can be derived from the well-known scheelite structure adopted by $CaWO_4$ and $CaMoO_4$. Further, while $Na_{0.25}MoO_3$ is

* Corresponding author. Tel.: (65) 6874 2956. Fax: (65) 6777 6126. E-mail: phychowd@nus.edu.sg.
[†] National University of Singapore.
[‡] Nanyang Technological University.

(1) Guyomard, D.; Sigala, C.; Salle, A. L. G. L.; Piffard, Y. *J. Power Sources* **1997**, *68*, 692.
(2) Poizot, P.; Baudrin, E.; Laruelle, S.; Dupont L.; Touboul, M.; Tarascon, J.-M. *Solid State Ionics* **2000**, *138*, 31.
(3) Denis, S.; Baudrin, E.; Orsini, F.; Ouvrard, G.; Touboul, M.; Tarascon, J.-M. *J. Power Sources* **1999**, *81−82*, 79.
(4) Leroux, F.; Piffard, Y.; Ouvrard, G.; Mansot, J.-L.; Guyomard, D. *Chem. Mater.* **1999**, *11*, 2948.
(5) Hara, D.; Shirakawa, J.; Ikuta, H.; Uchimoto, Y.; Wakihara, M.; Miyanaga, T.; Watanabe, I. *J. Mater. Chem.* **2002**, *12*, 3717.
(6) Hara, D.; Ikuta, H.; Uchimoto, Y.; Wakihara, M. *J. Mater. Chem.* **2002**, *12*, 2507.
(7) Hara, D.; Shirakawa, J.; Ikuta, H.; Uchimoto, Y.; Wakihara, M.; Miyanaga, T.; Watanabe, I. *J. Mater. Chem.* **2003**, *13*, 897.
(8) Martos, M.; Morales, J.; Sanchez, L. *J. Mater. Chem.* **2002**, *12*, 2979.
(9) Nazar, L. F.; Goward, G.; Leroux, F.; Duncan, M.; Huang, H.; Kerr, T.; Gaubicher, J. *Intl. J. Inorg. Mater.* **2001**, *3*, 191.
(10) Leroux, F.; Nazar, L. F. *Solid State Ionics* **2000**, *133*, 37.
(11) Leroux, F.; Goward, G. R.; Power, W. P.; Nazar, L. F. *Electrochem. Solid-State Lett.* **1998**, *1*, 255.
(12) Kim, S. S.; Ogura, S.; Ikuta, H.; Uchimoto, Y.; Wakihara, M. *Chem. Lett.(Japan)* **2001**, 760.
(13) Kim, S. S.; Ogura, S.; Ikuta, H.; Uchimoto, Y.; Wakihara, M. *Solid State Ionics* **2002**, *146*, 249.
(14) Wakihara, M.; Ikuta H.; Uchimoto Y. *Advances in Lithium-Ion Batteries*; Schalkwijk, W. A. V., Scrosati, B., Eds.; Kluwer Academic/Plenum Publishers: New York, 2002; p 103.

10.1021/cm0348287 CCC: $27.50
Published on Web 12/25/2003

a mixed (good electronic and ionic) conductor, MoO_3, $CaMoO_4$, and $MnMoO_4$ are electronic insulators. This necessitated Kim et al.[12,13] during their studies, to use as much as 40 wt. % of acetylene black as the conducting additive to fabricate the electrodes with $MnMoO_4$.

Presently, we report on the synthesis and electrochemical behavior of the compound $CaMoO_4$. Two interesting aspects motivated our study. First, the compound can be precipitated in nanocrystalline form, without any water of hydration from aqueous salt solutions at room temperature (RT = 27 °C). This afforded a method of coating the particles with conducting carbon during the RT synthesis. Second, our recent studies on the electrochemical properties of Ca-containing compounds $CaSnO_3$,[15,16] $(Ca,Li)(Fe,Sn)O_4$,[17] $Ca_2Fe_2O_5$, and $Ca_2Co_2O_5$[18] definitely showed the beneficial effect of the "spectator" Ca ion to deliver high and reversible capacities vs Li at least up to 50 charge−discharge cycles. Indeed, Ca plays a similar role in the present case, and reversible capacities of 440−500 mA h/g with >98% Coulombic efficiency up to 50 cycles have been observed for the 10% C-coated $CaMoO_4$.

Experimental Section

Solution precipitation and sol gel methods have been used for the synthesis of $CaMoO_4$. For the solution precipitation method,[19] a 0.08 M solution of $CaCl_2$ (Merck) in deionized water was added dropwise to the 0.16 M aqueous solution of Li_2MoO_4 (Alfa Aesar) with stirring and heating to 60 °C on a hot plate to ensure complete precipitation to yield 15.8 g of $CaMoO_4$. The precipitate was washed several times with deionized water to remove soluble impurities and was recovered by filtration. The product was dried at 160 °C for 24 h in an oven. The carbon (C) coating was done on $CaMoO_4$ grains following the aforementioned solution precipitation method, except that Super P MMM carbon (ENSACO) was well-dispersed in the Li_2MoO_4 solution prior to addition of the $CaCl_2$ solution, in two proportions in separate batches [5 and 10 wt % with respect to weight of the expected yield (∼16.3 g) of $CaMoO_4$]. This procedure is similar to that adopted by Yang et al.[20] for the carbon coating on MnO_2. The product was filtered and dried as above.

For the sol−gel synthesis, the citrate complex method[15] was adopted: 0.25 M citric acid (Fischer) was dissolved in 1 M of ethylene glycol (Merck) at 50 °C, followed by the addition of $CaCO_3$ (0.025 M; Merck). After complete dissolution of the latter, 0.025 M of MoO_2 (Aldrich) dissolved in minimum amount of 15% H_2O_2 was then added. The sol thus formed was heated at 135 °C for 12 h to obtain a deep-brown gelatinous mass. It was then decomposed by heating at 350 °C for 4 h in air. The black flaky product obtained was crushed to a fine powder and heated at 500 °C for 6 h in air to obtain crystalline $CaMoO_4$ (4.9 g).

For crystallographic analysis, powder X-ray diffraction (XRD) patterns were collected using a Siemens D5005 diffractometer equipped with Cu Kα radiation. Morphological studies were conducted using SEM (JEOL JSM-6700F, field emission electron microscope) and TEM (JEOL JEM 3010 operating at 300 kV). For SEM, the samples were coated with platinum to minimize charging effects. For TEM, the powder was dispersed in methanol and a drop of suspension deposited on a holey carbon-coated Cu-grid. The carbon contents of the materials were determined by thermogravemetric analysis (TGA) (TA Instruments SDT2960 simultaneous DTA−TGA) from RT to 800 °C with a heating rate of 5 °C/min in air. Composite electrodes for the electrochemical studies were prepared with the active material, Super P carbon, and binder (Kynar 2801) in the weight ratios 80:10:10 ($CaMoO_4$, solution precipitation), 70:15:15 (C-coated $CaMoO_4$), and 65:20:15 ($CaMoO_4$, sol−gel). These are optimized compositions to obtain good composite electrodes with reproducible results. A thick slurry of the respective mixture was made using 1-methyl 2-pyrrolidone (NMP) as the solvent and coated onto copper foil by the doctor blade technique. The thick film (20−30 μm) electrodes were dried at 80 °C in an air oven, pressed between twin rollers, and cut into circular disks (16 mm) followed by drying in a vacuum oven at 70 °C for 12 h. These were then transferred to an Ar-filled glovebox which maintains <1 ppm of H_2O and O_2 (MBraun, Germany). Coin cells (size 2016) were fabricated in the glovebox with Li metal (Kyokuto Metal Co., Japan) foil as counter electrode, Celgard 2502 membrane as the separator, and 1 M $LiPF_6$ in ethylene carbonate (EC) and diethyl carbonate (DEC) (1:1 by volume, Merck Selectipur LP40) as the electrolyte. The active material content in the cells is ∼6 mg. The cells were aged for 24 h before testing. The cyclic voltammetry and galvanostatic charge−discharge cycling of the cells were done at RT by computer-controlled MacPile II (Biologic) and Bitrode multiple battery testers (model SCN, Bitrode).

Results and Discussion

Structural Characterization. The powders of $CaMoO_4$ are crystalline and white, whereas the 5 and 10 wt % C-coated $CaMoO_4$ are black. An estimation of the carbon content for the 10 wt % C-coated $CaMoO_4$ and the sol−gel $CaMoO_4$ was made by TGA analysis. There was no weight loss until 500 °C in both the samples, indicating that there is no water of hydration. Major weight loss in the C-coated $CaMoO_4$ started above 500 °C and was complete at 680 °C, due to oxidation of C. Its content was calculated to be 11.8% of the sample weight. This is slightly larger than the 10 wt % expected and must be due to incomplete precipitation of $CaMoO_4$ from the solution. A similar argument applies to the 5 wt % C-coated $CaMoO_4$. The TGA of the sol−gel $CaMoO_4$ showed only a weight loss of 0.33% in the temperature range of 600−650 °C. This reveals the presence of amorphous carbon in trace amounts in the sol−gel $CaMoO_4$ due to the residue from the citrate complex.

The XRD patterns of $CaMoO_4$ synthesized by sol−gel and solution precipitation (soln ppt) and carbon-coated methods are shown in Figure 1. The diffraction lines of pattern i in Figure 1a are slightly shifted to higher 2θ values in comparison to pattern ii. This is due to the different method of synthesis. On the other hand, the lines of pattern i in Figure 1a are rigorously superimposable on those in Figure 1b. All peaks can be assigned to those reported for $CaMoO_4$ in the JCPDS file (no. 77-2239). This confirms the formation of the phase-pure compounds, at least to the detection limit (<2 or 1%) of XRD. Since the Super P carbon is amorphous and its content is small, it is not observed in the XRD patterns of the C-coated $CaMoO_4$. The $CaMoO_4$ crystal-

(15) Sharma, N.; Shaju, K. M.; Subba Rao, G. V.; Chowdari, B. V. R. *Electrochem. Commun.* **2002**, *4*, 947.
(16) Sharma, N.; Shaju, K. M.; Subba Rao, G. V.; Chowdari, B. V. R. In *Solid State Ionics: Trends in The New Millennium*; Chowdari, B. V. R., Prabaharan, S. R. S., Yahaya, M., Talib, I. A., Eds.; World Scientific: Singapore, 2002; p 87.
(17) Sharma, N.; Shaju, K. M.; Subba Rao, G. V.; Chowdari, B. V. R. *J. Power Sources* **2003**, *124*, 204.
(18) Sharma, N.; Shaju, K. M.; Subba Rao, G. V.; Chowdari, B. V. R. *Electrochim. Acta* (in press).
(19) Sen, A.; Pramanik, P. *Mater. Lett.* **2001**, *50*, 287.
(20) Yang, X.; Tang, W.; Liu, Z.; Makita, Y.; Kasaishi, S.; Ooi, K. *Electrochem. Solid-State Lett.* **2002**, *5*, A191.

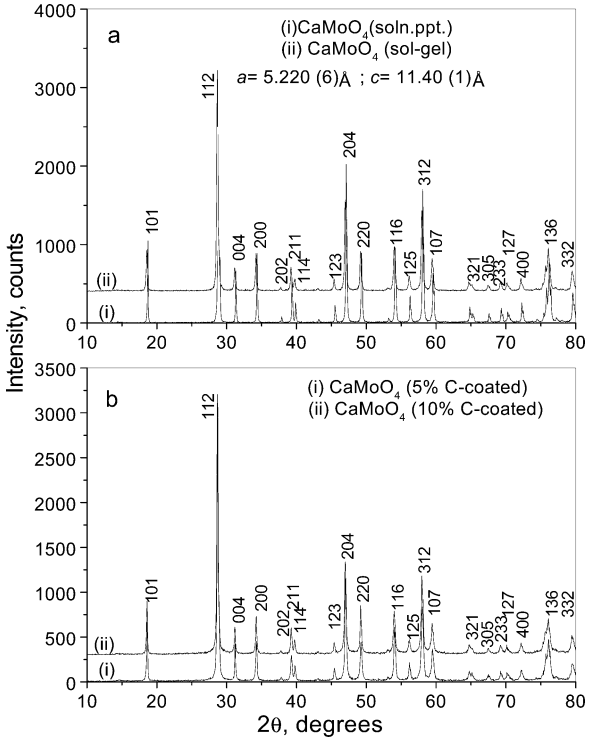

Figure 1. Powder X-ray diffraction (XRD) patterns of (a) $CaMoO_4$ (solution precipitated) and $CaMoO_4$ (sol−gel); (b) 5% and 10% C-coated $CaMoO_4$. Miller indices (*hkl*) and tetragonal lattice parameters (*a*, *c*) are shown.

lizes in the mineral scheelite structure[21,22] (tetragonal, space group I_1/a) with the primitive cell comprising Ca^{2+} ions and $(MoO_4)^{2-}$ tetrahedra with two formula units.[22] The tetragonal lattice parameters, derived by the least-squares fitting of the 2θ and *hkl* values, are given in Figure 1 and are in agreement with the JCPDS file [a = 5.200(5) Å, c = 11.365(3) Å].

The SEM photographs (Figure 2a−c) of the compounds clearly depict that morphology is dependent upon the synthetic method. The soln ppt $CaMoO_4$ showed large agglomerates (7−10 μm) of fine particles (Figure 2a). The in-situ C-coating during the precipitation of $CaMoO_4$ leads to uniform and smooth particles of 1−2 μm size (Figure 2b), revealing that the coating prevents the agglomeration of the small crystallites into bigger units. The sol−gel $CaMoO_4$ shows the formation of well-separated nanocrystallites with size in the range of 50−80 nm (Figure 2c). The bright field TEM photographs reveal that the primary agglomerates of soln ppt $CaMoO_4$ are comprised of nanocrystallites (size 50−150 nm) (Figure 3a). These nanoparticles are interlocked randomly to form large agglomerates. The TEM of C-coated $CaMoO_4$ shows very uniform nanocrystallites with a size of only 50−80 nm (Figure 3b). Thus, carbon coating results in uniform crystallites with reduced size consistent with the SEM observations. The TEM lattice images observed on individual crystallites of the soln ppt and C-coated $CaMoO_4$ (Figure 3c,d) reveal perfect order at the unit cell scale. The *d* spacing of the lattice fringes (Figure 3c) is 3.1 Å and corresponds to the (112)

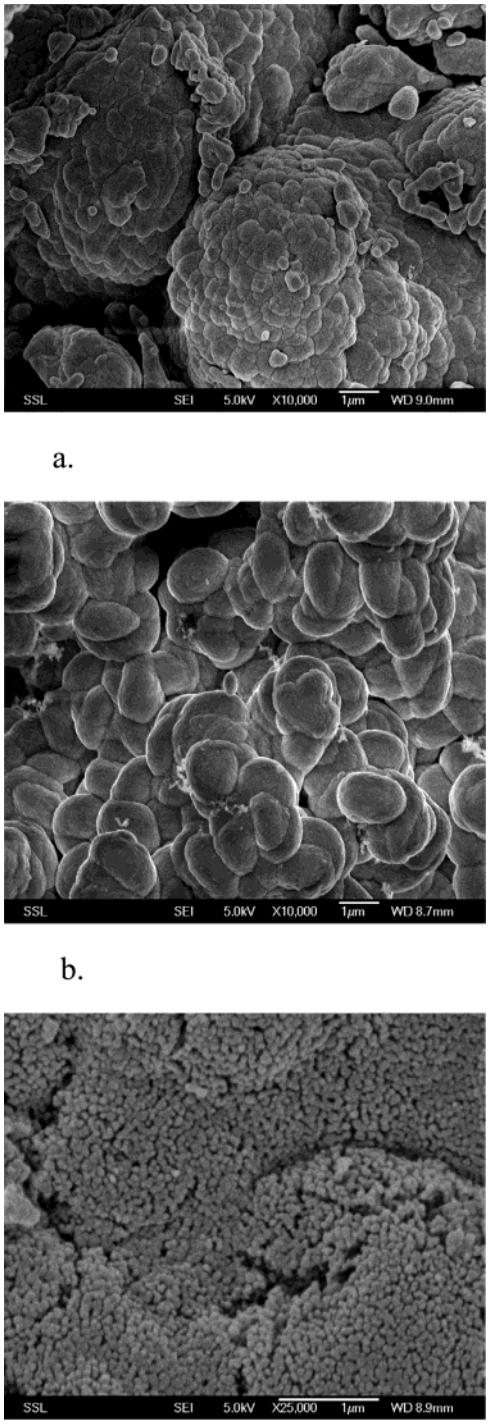

Figure 2. SEM photographs of the powders of $CaMoO_4$: (a) solution precipitated, (b) 10% C-coated, and (c) sol−gel synthesized.

plane. Overlap of two or more crystallites due to the agglomeration of nanocrystals is also seen, in upper right side of Figure 3c. Further, TEM of the C-coated sample (Figure 3d) reveals that the carbon is coated as a uniform layer, amorphous in nature, on the surface of $CaMoO_4$ with thickness 8−12 nm over the crystalline grains of $CaMoO_4$.

Galvanostatic Cycling. The electrochemical performance of pure and C-coated $CaMoO_4$ vs Li was examined and compared under galvanostatic cycling conditions at room temperature. The first cycle always

(21) Cho, W.-S.; Yashima, M.; Kakihana, M.; Kudo, A.; Sakata, T.; Yoshimura, M. *J. Am. Ceram. Soc.* **1997**, *80*, 765.
(22) Simon, J.; Banys, J.; Hoentsch, J.; Volkel, G.; Bottcher, R.; Hofstaetter, A.; Scharmann, A. *J. Phys.: Cond. Matter* **1996**, *8*, L359.

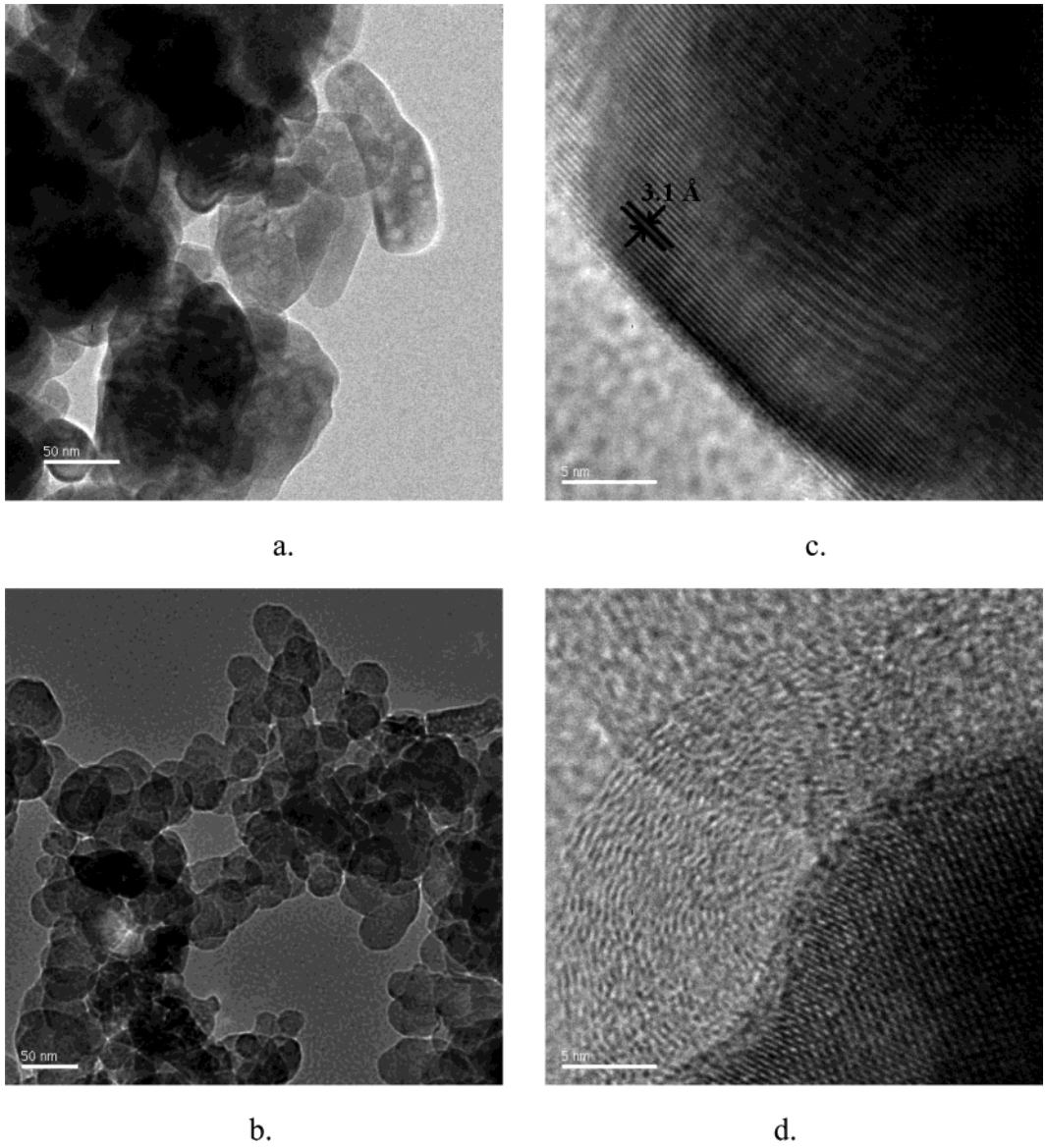

Figure 3. TEM photographs of $CaMoO_4$: (a) solution precipitated and (b) 10% C-coated (scale: white bar measures 50 nm). High-resolution lattice images of $CaMoO_4$: (c) solution precipitated and (d) 10% C-coated (scale: white bar measures 5 nm). In part c, the lattice spacings correspond to the (112) planes with a *d* spacing of 3.1 Å. In part d, the amorphous nature of the coated carbon is clearly delineated from the crystalline region of $CaMoO_4$. See the text.

commenced cathodically from the open circuit voltage (OCV) condition. In galvanostatic cycling, the first two discharge−charge cycles were carried out at a current rate of 10 mA/g and the rest at 60 mA/g up to 50 cycles. Figure 4 shows the voltage profiles corresponding to the first-discharge reaction from OCV to 0.005 V and the subsequent charge cycle up to 2.5 V. The voltage drops rapidly up to 0.8 V, followed by a sloping profile until the lower cutoff limit of 0.005 V for the $CaMoO_4$ (soln ppt). The voltage profile of $CaMoO_4$ (sol−gel) (Figure 4b) shows a plateau, at a voltage ∼0.9 V, till a capacity of 375 mA h/g is reached. After this, the sloping region sets in and extends to 0.005 V to give a total discharge capacity of 853 mA h/g. The voltage profile of 10% C-coated $CaMoO_4$ (Figure 4c) comprises a flat region at ∼0.85 V after an initial drop from OCV. After reaching a discharge capacity of 100 mA h/g, there is a sloping profile up to almost 650 mA h/g, followed by steeper voltage drop till 0.005 V. The capacity contribution from the latter sloping region is ∼375 mA h/g, so the total discharge capacity is 1025 mA h/g. A similar behavior was shown by 5% C-coated $CaMoO_4$ with a total capacity of 922 mA h/g.

The first-discharge curves shown in Figure 4b,c exhibit the voltage plateau at 0.85−0.9 V vs Li. Kim et al.[12,13] also have observed a voltage plateau at ∼0.8 V, followed by a sloping profile with another plateau at ∼0.3 V and continuous decrease of voltage till 0 V for $MnMoO_4$ studied as cathode vs Li. This is expected, since both the compounds, $CaMoO_4$ and $MnMoO_4$, contain MoO_4 tetrahedra and are structurally related. The plateau at 0.8−0.9 V may be due to the breakdown of the metal oxide framework catalytically enhanced by carbon. A voltage plateau at ∼0.5−0.8 V has also been observed by Leroux et al.[10,11] during the first discharge in $Na_{0.25}MoO_3$, in which Mo ion adopts an octahedral coordination. Thus, slight differences in the voltage plateau values arise due to the crystal structure, the nature of the spectator ion (Ca or Mn), O-coordination of the active ion, and, possibly, the nanoparticle nature

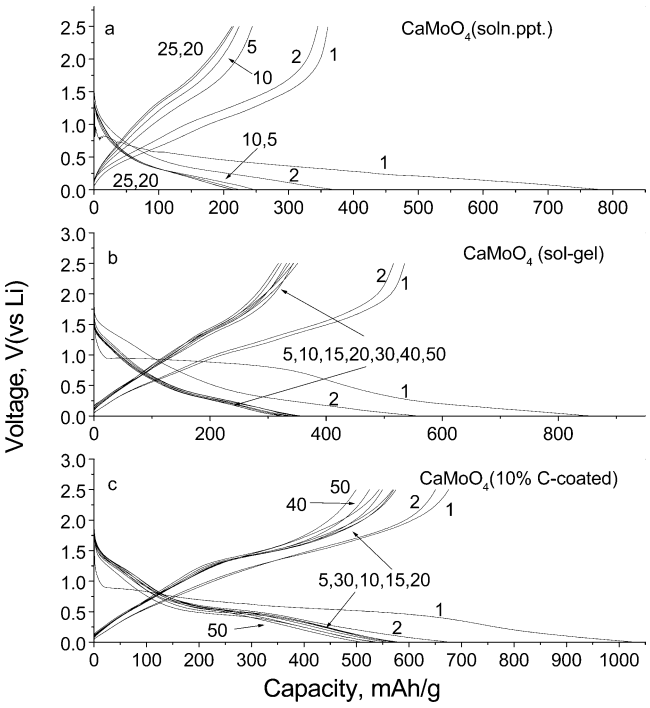

Figure 4. The voltage vs capacity profiles in the voltage window 0.005−2.5 V for (a) $CaMoO_4$ (solution precipitated), 1−25 cycles; (b) $CaMoO_4$ (sol−gel), 1−50 cycles; and (c) $CaMoO_4$ (10% C-coated), 1−50 cycles. The first two cycles were performed at a current density of 10 mA/g and during 5−50 cycles at 60 mA/g. Only select cycles are shown. The numbers refer to cycle numbers. The capacity values are uncorrected for carbon contribution.

of the compound. Similar variations were observed by us and others in tin-based oxides[15,16,23,24] and in pure and mixed transition metal oxides.[17,18,25]

The first-charge curves, up to 2.5 V shown in Figure 4, for all the $CaMoO_4$ compounds are smooth up to ∼2 V with a slight indication of a plateau at 1.3−1.5 V in 10% C-coated $CaMoO_4$. Above 2 V, the voltage rises rapidly, except for the C-coated $CaMoO_4$, indicating little capacity above this voltage. These first-charge curves are almost identical to the one observed in $MnMoO_4$.[12−14] The first-charge capacities (mA h/g) are as follows: $CaMoO_4$ (soln ppt), 361; $CaMoO_4$ (sol−gel), 535; 10% C-coated $CaMoO_4$, 680. This shows that the latter compound performs better. The second-discharge profiles differ significantly from those of the first discharge indicating that the mechanism of operation is different in this case, and as expected, the capacities are also smaller. In addition, the profile of 10% C-coated $CaMoO_4$ shows a plateau at ∼0.5 V, identical to that noted in $MnMoO_4$.[12−14] Subsequent charge−discharge cycles at 60 mA/g show excellent overlap of the respective profiles for sol−gel and 10% C-coated $CaMoO_4$. The Coulombic efficiency is >98%. During the 3−50 cycles, the following features are also clear: for $CaMoO_4$ (soln ppt), reversible capacities vary from 200 to 250 mA h/g and there is an increase in the electrode polarization from the 2nd cycle onward. The voltage plateau at 1.3−1.5 V in the charge curves appears only as a shoulder. For $CaMoO_4$ (sol−gel), reversible capacities vary from 300 to350 mA h/g and only small electrode polarization is seen. The voltage plateaus at 1.3−1.5 V in the charge curves and at 0.3−0.5 V in the discharge curves are discernible. For 10% C-coated $CaMoO_4$, high reversible capacities vary from 500 to 580 mA h/g with little electrode polarization from the 3rd cycle onward, and there are clear-cut voltage plateaus at 1.4−1.5 V in the charge curves and at 0.5−0.6 V in the discharge curves. These plateaus indicate a multiphase reaction involving Mo oxide in two or more low-valence states. The profiles of the 5% C-coated $CaMoO_4$ are similar to those of the 10% C-coated ones, except that the reversible capacities are smaller. Despite the nanoparticle nature of the various $CaMoO_4$ studied here, the superior performance of the 10% C-coated $CaMoO_4$ is definitely due to the improved electronic conductivity between the particles of $CaMoO_4$ and hence the better electronic transfer between the nanoparticles.

The voltage−capacity profiles shown in Figure 4 include the contribution from the Super P carbon used as conducting additive during fabrication of the electrodes, both uncoated and coated $CaMoO_4$. We have separately determined the voltage−capacity profiles of Super P carbon vs Li, and the first-discharge and reversible charge−discharge capacities were found to be 457 and 180 mA h/g in the voltage range of 0.005−2.0 V up to 25 cycles. Accordingly, from the known weights of the active material and Super P carbon in the composite electrodes (see Experimental Section), we have subtracted the capacity contribution of the carbon from the observed capacities during all the discharge−charge cycles for all the compositions of $CaMoO_4$, including the C-content of the coated ones. These corrected capacity values are given in Table 1 and plotted in Figure 5 as a function of the cycle number.[26] The moles of Li participating in the charge−discharge reactions, calculated from the molecular weight and the corrected capacity values, are also given in Table 1.

The theoretically expected capacity value for the first discharge involving crystal structure destruction and reduction of the Mo^{6+} to Mo^0 in $CaMoO_4$ is 804 mA h/g (6 mol of Li). The Ca^{2+} ion in $CaMoO_4$ is not expected to be reduced to Ca metal under room-temperature electrochemical conditions. This can be understood by a consideration of free energies of formation,

(23) Behm, M.; Irvine, J. T. S. *Electrochim. Acta* **2002**, *47*, 1727.
(24) Li, N.; Martin, C. R. *J. Electrochem. Soc.* **2001**, *148*, A164.
(25) Poizot, P.; Laruelle, S.; Grugeon, S.; Dupont, L.; Tarascon, J.-M. *Nature* **2000**, *407*, 496.

(26) Leroux and Nazar[10] in their studies on Na_xMoO_3 pointed out that the carbon black used as a conducting additive to these mixed oxide composite electrodes has a catalytic interfacial-enhancement effect, and thus, a simple subtraction of the carbon contribution according to its relative weight percentage from the total observed electrode capacity to obtain the reversible capacity is not strictly accurate. They proposed an equation for evaluating the corrected reversible capacity, Q_{rev} (composite): Q_{rev}(composite) = Q_{rev}(experimental)/(1 + X_C%), where X_C% is the relative weight percentage of the carbon. But, they also noted that since the carbon black has a reversible capacity 5 times less than that of the composite, the corrected capacity Q_{rev} (composite) of Na_xMoO_3 is underestimated by using the above equation. In the present study, the Super P carbon has a reversible capacity about 3 times less than that of the $CaMoO_4$ composite. By using the above method of correction to the observed capacities, we find that the values listed in Table 1 and shown in Figure 5 are higher by about 1−7% for all the compositions. For example, the 10% C-coated $CaMoO_4$, which has a total carbon content of 25 wt % in the composite electrode, showed uncorrected first-charge capacity of 680 mA h/g. After correction as above, the value is 544 mA h/g compared to the 582 mA h/g listed in Table 1. Thus, both methods of correction to the Q_{rev}(experimental) for all the compositions agree within a few percent.

Table 1. Charge and Discharge Capacities (mA h/g) and the Corresponding Moles of Li Per Formula Unit for $CaMoO_4$[a]

$CaMoO_4$ (weight ratio)[b]	upper cutoff voltage (lower, 0.005 vs Li) V	capacity, mA h/g (mol of Li) at 10 mA/g 1st discharge	at 10 mA/g 1st charge	at 60 mA/g 20th discharge	at 60 mA/g 20th charge	at 60 mA/g 50th discharge	at 60 mA/g 50th charge
soln ppt (80:10:10)	2.5	758 (5.7)	339 (2.5)	190 (1.4)	188 (1.4)		
sol−gel (65:20:1 5)	2.0	718 (5.4)	450 (3.4)	284 (2.1)	281 (2.1)	261 (2.0)	255 (1.9)
	2.5	713 (5.3)	480 (3.6)	268 (2.0)	267 (1.9)	292 (2.1)	289 (2.1)
	3.0	739 (5.5)	494 (3.7)	264 (2.0)	259 (1.9)		
5 wt % C-coated (70:15:15)	2.5	794 (5.9)	493 (3.7)	401 (2.9)	398 (2.9)		
10 wt % C-coated (70:15:15)	2.0	895 (6.7)	552 (4.2)	447 (3.3)	444 (3.3)	343 (2.6)	336 (2.5)
	2.5	853 (6.4)	582 (4.3)	508 (3.8)	502 (3.8)	439 (3.3)	431 (3.2)
	3.0	805 (6.0)	584 (4.4)	479 (3.6)	471 (3.5)		

[a] Corrected for the carbon content in the uncoated as well as carbon-coated composite electrodes. [b] Active material:carbon:binder

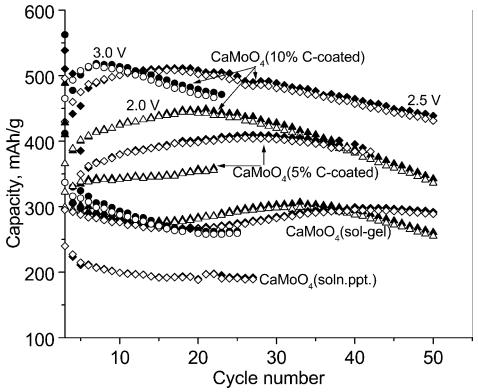

Figure 5. The charge−discharge capacities (corrected for uncoated and coated carbon contribution) as a function of cycle number (3−50 cycles) for solution precipitated, sol−gel, 5% C-coated, and 10% C-coated $CaMoO_4$ at a current density of 60 mA/g. Upper cutoff voltages are indicated by the symbols △ (2.0 V), ◇ (2.5 V), ○ (3.0 V). In all cases the lower cutoff voltage is 0.005 V vs Li. Filled and open symbols indicate discharge and charge capacities, respectively.

$[\Delta G_f^0(298K)]$. The value of CaO (−144.37 kcal/mol) is more negative than that of Li_2O (−134.13 kcal/mol).[27] Indeed, our studies on $CaZrO_3$ vs Li have shown that neither Ca^{2+} nor Zr^{4+} can be reduced to the respective metals under room-temperature electrochemical conditions.[28] However, this argument does not apply to transition-metal oxides, which can exhibit different valence states of the metal ion. Thus, even though ΔG_f^0(298K) for MoO_3 and MoO_2 are −159.66 and −127.40 kcal/mol respectively,[27] $Mo^{6+}O_3$ can be readily reduced to lower valent oxide by Li to give $Li_xMo^{6+/5+}O_3$ ($x < 1$) at room temperature under both chemical and electrochemical conditions.[10,11,29] The observed first-discharge capacity for the 10% C-coated $CaMoO_4$ is slightly higher than the theoretical value, by 0.4 mol of Li, whereas for the 5% C-coated $CaMoO_4$ there is good agreement (5.9 vs 6.0 mol of Li). The capacity values for the soln ppt and sol−gel $CaMoO_4$ are less than the theoretical values by ∼6−12% (Figure 5 and Table 1), indicating that Mo^{6+} was not reduced to metal (Mo^0) but only to a lower oxidation state and/or the discharge reaction was incomplete, possibly due to the insulating nature of $CaMoO_4$. The first-charge capacities, with the upper cutoff voltage at 2.5 V, correspond to 4.3, 3.7, 3.6, and 2.5 mol of Li respectively for 10% C-, 5% C-coated, sol−gel, and soln ppt $CaMoO_4$. Thus, the irreversible capacity loss (ICL) remains the same, 2.15 ± 0.05 mol of Li for the 5 and 10% C-coated $CaMoO_4$, whereas the ICL is only 1.7 mol of Li for sol−gel but as high as 3.2 mol of Li for soln ppt $CaMoO_4$. Part of the ICL is contributed by the solid electrolyte interface (SEI) formation on the oxide, including the C-coated $CaMoO_4$, and the rest must exist as electrochemically inactive Li_2O. During the 3−50 cycles, performed at a higher current rate of 60 mA/g in the range of 0.005−2.5 V, the observed capacities are smaller than those obtained during the first two cycles, which were carried out at 10 mA/g. For the sol−gel sample and 10% C-coated $CaMoO_4$, cycling was also performed with the upper cutoff voltages 2.0 and 3.0 V. Select values are given in Table 1 and plotted in Figure 5. As can be expected, the first-charge cycle capacities are about ∼6% smaller with 2.0 V cutoff as compared to the values with 2.5 V cutoff. With an upper cutoff of 3.0 V, the capacities are almost the same for 10% C-coated $CaMoO_4$ but 3% higher for sol−gel $CaMoO_4$. The trend of variation of the charge and discharge capacities with the cycle number for 10% C-coated $CaMoO_4$ is exactly the same with the upper cutoff voltages 2.0 and 2.5 V. However, with the cutoff voltage of 3.0 V, the capacities started fading much earlier, from the ninth cycle onward. For sol−gel $CaMoO_4$, with the cutoff voltage of 3.0 V, the initial higher capacities decrease up to 18 cycles and stabilize at ∼260 mA h/g in the range of 20−25 cycles. Therefore, we conclude that the optimum working voltage is 0.005−2.5 V in $CaMoO_4$.

The influence of the preparation method and C-coating on the cycling performance is clearly brought out in the data of Table 1 and Figure 5. For the soln ppt $CaMoO_4$, the third cycle capacity of 240 mA h/g decreases to 190 mA h/g at the 15th cycle and remains stable up to 27 cycles. This value corresponds to recyclable Li of only 1.4 mol. The Coulombic efficiency is ∼99%. For sol−gel $CaMoO_4$ the third cycle capacity is 295 mA h/g, which decreases by about 10% at the end of 20 cycles, but then increases slowly to 296 mA h/g up to 35 cycles and stabilizes at this value (±5 mA h/g) up to 50 cycles (Figure 5). This corresponds to 2.1 mol

(27) *CRC Handbook of Chemistry and Physics*, 67th ed.; Weast, R. C., Ed.; CRC Press, Inc., Boca Raton, FL, 1986−1987; pp D57−75.
(28) Sharma, N.; Shaju, K. M.; Subba Rao, G. V.; Chowdari, B. V. R. *Solid State Ionics* (submitted).
(29) Iriyama, Y.; Abe, T.; Inaba, M.; Ogumi, Z. *Solid State Ionics* **2000**, *135*, 95.

of Li, and the Coulombic efficiency is ~99%. The C-coated $CaMoO_4$ exhibits consistently higher initial capacities that slowly increase up to 17−25 cycles. The capacity remains stable at ~400 mA h/g (2.9 mol of Li) in the range of 20−40 cycles for the 5% C-coated $CaMoO_4$. For the 10%-C-coated $CaMoO_4$, the 20th cycle-discharge capacity is 508 mA h/g (cutoff voltage, 2.5 V). This corresponds to 3.8 mol of recyclable Li. However, the capacity decreases in the range 20−50 cycles and is 439 mA h/g at the end of 50th discharge-cycle for the 10% C-coated $CaMoO_4$. The Coulombic efficiencies are ~99% for both 5% and 10% C-coated $CaMoO_4$. The increasing trend in the charge and discharge capacities in the range of 3−20 cycles for the C-coated $CaMoO_4$ may be attributed to the "activation" of the electrode. While the C-coating enhances interparticle electronic conductivity, it may prevent the full participation of the active material in these initial cycles, especially because crystal structure destruction is involved in the first discharge. A similar trend of activation of the electrode has been noted by us[15,16] in the cycling behavior of nano-$CaSnO_3$. Nearly stable performance is observed with 5% C-coated $CaMoO_4$ from 20 to 40 cycles, but lower capacity values are showed, as against 10% C-coated $CaMoO_4$. However, in this range (20−40 cycles), the capacity fading is larger for 10% C-coated $CaMoO_4$. This indicates that optimum carbon coating, with respect to high achievable capacities at the current rate of 60 mA/g and stable cycling performance, is between 5 and 10 wt %.

A comparison of the cycling performance of C-coated $CaMoO_4$ (Figure 5 and Table 1) with the results reported by Kim et al.[12,13] for $MnMoO_4$ shows that $CaMoO_4$ performs better. A first-charge capacity of 1000 mA h/g in $MnMoO_4$ was found to decrease continuously to ~400 mA h/g after 25 cycles in the voltage range of 0−2.0 V at the current rate 0.2 mA/cm^2. Further, the authors employed 40 wt % of conducting carbon in the composite electrode, and its contribution to the observed capacity will be considerable. Thus, the Ca ion is a superior "spectator" compared to Mn ion in the Mo−O matrix, and C coating has a positive influence. The beneficial role of Ca ions in other oxide matrixes (Sn, Fe, Co) has been shown by us previously.[15−18,28]

Cyclic Voltammetry. Cyclic voltammetry (CV) is a complimentary technique to galavanostatic cycling in giving information on the possible mechanism of operation of the electrode. The CV profiles of the various $CaMoO_4$ compositions were recorded at room temperature in the voltage range of 0.005−2.5 V vs Li at a sweep rate of 0.058 mV/s up to 25 cycles. For clarity, select cycles only are shown in Figure 6. The CV plots differ from each other and highlight the influence of morphology and C-coating on the electrochemical performance of $CaMoO_4$. The first-discharge sweep, commenced cathodically from OCV to 0.005 V, is at variance from the subsequent discharge curves, revealing that the first-discharge reaction differs from the rest. Here, the material is transformed into an amorphous composite CaO, Li_2O, and "Li_xMoO_y". The first-discharge curve for soln ppt $CaMoO_4$ shows a small reduction peak at ~0.75−0.8 V and $|\Delta Q|$ increases continuously till 0.005 V (Figure 6a). Subsequent charge−discharge cycles are almost featureless, and the areas under the cathodic and anodic regions decrease upon cycling, indicating capacity fading. This must be due to incomplete participation of the active material, due to its highly insulating nature and bigger particle-morphology. The first-discharge sweep for sol−gel $CaMoO_4$ (Figure 6b) comprises a broad peak centered around 0.5 V, followed by a gradual increase in $|\Delta Q|$ down to 0.005 V. The first-charge sweep shows three small peaks, around 0.65, 1.2, and 1.6 V, of equal intensity. The second discharge profile shows a broad shoulder around 1.25 V and then $|\Delta Q|$ increases till 0.005 V. The fifth discharge profile shows an indication of peak formation in the low-voltage region, ~0.25 V. The subsequent charge−discharge profiles are qualitatively similar, except for the diminishing peak intensities and their areas up to 25 cycles.

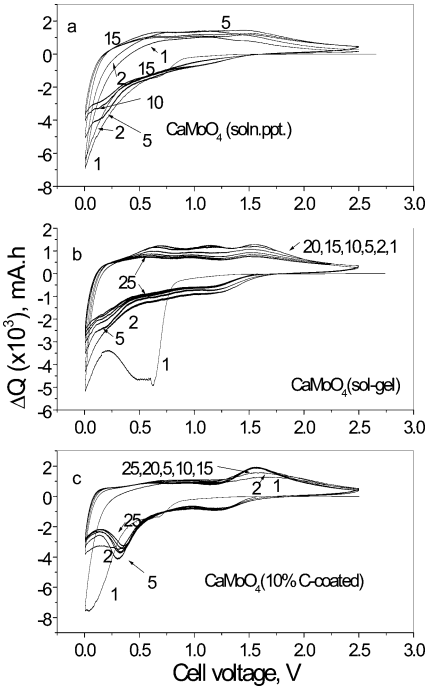

Figure 6. Cyclic voltammograms of (a) solution precipitated, (b) sol−gel, and (c) 10% C-coated $CaMoO_4$. Li metal was the counter and reference electrode. The scan rate was 0.058 mV/s. The voltage window was 0.005−2.5 V. Only select cycles are shown. The numbers refer to cycle numbers.

The first-discharge sweep in the CV of 10% C-coated $CaMoO_4$ (Figure 6c) shows a small peak at ~0.6 V, followed by a continuous increase in the $|\Delta Q|$ values up to 0.005 V. Subsequent charge sweeps show a peak developing around 1.55 V. The second and subsequent discharge curves show a broad peak around 1.2 V, and the main reduction peak occurs at ~0.3 V. These correspond well to the plateau regions noted in galvanostatic profiles (Figure 4c). The corresponding charge cycles show a clear peak at 1.55−1.60 V, which increases in intensity up to 25 cycles. The increase in the peak intensity upon cycling can be attributed to the completion of the structure-destruction process spreading over these initial cycles, after which the nanocrystalline material participates fully in the electrochemical cycling. The well-defined peaks observed in the charge−discharge cycles in C-coated $CaMoO_4$ can be attributed to the oxide bronze Li_xMoO_y formation at ~1.2 and 0.3 V during the discharge sweep (varying valence states of Mo ion) and its oxidation occurring around ~1.55 V

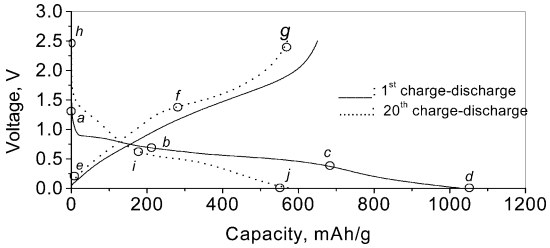

Figure 7. The voltage vs capacity profiles (first and 20th cycle) for $CaMoO_4$ (10% C-coated) in the voltage window of 0.005−2.5 V vs Li. The first cycle was at 10 mA/g and the 20th cycle at 60 mA/g (reproduced from Figure 4c).

in the charge sweep. The CV studies thus corroborate the galvanostatic cycling results.

Charge−Discharge Reaction Mechanism. The mechanism of the charge−discharge process in $CaMoO_4$ can be inferred from studies done on the related Mo oxide systems $MnMoO_4$[12−14] and $Na_{0.25}MoO_3$.[9−11] On the basis of in situ XRD, XANES, and NMR studies, it has been established that the first-discharge reaction is essentially a crystal structure destruction process yielding a highly disordered product comprising a mixture of an inert matrix, Li−M−O (M = Na or Mn as the matrix metal) and an electrochemically active "Li_xMoO_y" phase.[5−7,9−14] The formation of Li−M−O is irreversible and contributes to ICL. In the case of $MnMoO_4$, Kim et al.[12−14] did not find evidence of the formation of Mo metal during the first discharge (reduction by Li) up to 0 V but only reduction to a lower valence state, Mo^{1+} or Mo^{2+}. The Mn^{2+} ion in $MnMoO_4$ remained unreduced. On the other hand, studies on the system $Mn_{1-x}(Mo_xV_{1-x})_2O_6$ (x = 0 and 0.4) by Hara et al.[5−7] showed that on full discharge, Mn^{2+} and Mo^{6+} ions were reduced to Mn^0 and Mo^0 (metal) respectively, whereas V^{5+} was reduced to only V^{2+}. During the first charge and subsequent cycling, $Mo^0 \leftrightarrow Mo^{4+}$ and $V^{2+} \leftrightarrow V^{4+}$ occurs with the participation of Li ions.[5−7,12−14] To explain the observed high capacities in $MnMoO_4$, Kim et al.[12,13] invoked the participation of O ions (oxidation of O^{2-} and its reduction during charge and discharge, respectively) in addition to the Mo redox contribution. Electrochemical, NMR, and XAS studies on $Na_{0.25}MoO_3$[9−11] have shown that the Mo^{6+} ions get reduced to an average valence state of $Mo^{0.6+}$ during the first discharge. Formation of a highly oxygen deficient Li/Mo nanocomposite with a formula of "$Li_{5.28}MoO_{1.7}$" was proposed. Thus, the formation of Mo metal or otherwise during the first-discharge reaction depends on the crystal structure of the starting oxide, the matrix ion, and the presence or absence of another electrochemically active ion, e.g., V^{5+}, in addition to Mo ion.

Therefore, on the basis of the above reports on Mo compounds and galvanostatic cycling results for the 5- and 10% C-coated $CaMoO_4$, for which the first discharge capacity is in good agreement with the theoretical value of 6.0 mol of Li, of which 3.8 mol are recyclable for the latter composition, we propose a reaction mechanism involving the formation−decomposition of the oxide bronze "Li_xMoO_y". The first discharge profile (Figure 7, replotted from Figure 4c for clarity) for the 10% C-coated $CaMoO_4$ is divided into regions marked with boundaries *a*, *b*, *c*, and *d*. It shows an overall capacity of 1025 mA h/g, including the C contribution. The destruction of the crystal structure and amorphization of the nanoparticle $CaMoO_4$ occurs in the region *abc* with a small plateau at ∼0.85 V and a continuous decrease to 0.5 V consuming 3.5 mol of Li (475 mA h/g after correcting for C-content) as per eq 1.

$$CaMoO_4 + 3.5Li^+ + 3.5e^- \rightarrow CaO + 1.1Li_2O + Li_{1.3}Mo^{2.5+}O_{1.9} \quad (1)$$

At point *c*, $CaMoO_4$ has converted to the bronze "$Li_{1.3}Mo^{2.5+}O_{1.9}$". In the region *cd*, 2.5 mol of Li is consumed to form the bronze "$Li_{3.8}Mo^0O_{1.9}$" in which Mo attains a valency of 0 (eq 2).

$$Li_{1.3}Mo^{2.5+}O_{1.9} + 2.5Li^+ + 2.5e^- \leftrightarrow Li_{3.8}Mo^0O_{1.9} \quad (2)$$

The charge curve (*efg*, in the profile of 20th cycle) is almost a straight line up to point *f* and corresponds to the release of ∼2 mol of Li. This is the oxidation reaction (reverse of eq 2). However, the slope of the profile changes before the release of all 2.5 mol of Li, as suggested by eq 2. Thereafter, a small plateau sets in at ∼1.5 V, in the vicinity of point *f*, after which the profile shows a region of different slope (also seen as a broad shoulder in the first-charge curve, Figure 7). The region *fg* is attributed to the further oxidation of the bronze, releasing all 3.8 mol of Li at point *g* and forming "$Mo^{3.8+}O_{1.9}$" (eq 3).

$$Li_{1.3}Mo^{2.5+}O_{1.9} \leftrightarrow Mo^{3.8+}O_{1.9} + 1.3Li^+ + 1.3e^- \quad (3)$$

The small plateau region at ∼1.5 V may be the overlapping region between the reactions of eqs 2 and 3, signifying an equilibrium between the phases "$MoO_{1.9}$" and "Li_xMoO_y". The second and subsequent discharge cycles, which differ from the first-discharge reaction, also proceed in two steps, as indicated by the region *hij*. The sloping portion *hi*, contributes a capacity of 175 mA h/g (1.3 mol of Li), after correcting for the C-content (reverse of eq 3). This is followed by the plateau at ∼0.5 V, signifying the onset of the forward reaction of eq 2. The above mechanism in which charge−discharge cycling involves only 4.0 mol of Li (experimental, 3.8 Li), where Mo changes its valency from 0 to 4+, is consistent with the observations of the group of Wakihara on $MnMoO_4$[12−14] and Nazar on Na_xMoO_3,[10,11] who found that on charging to 2.0−3.5 V (vs Li), Mo adopts a valency of only 4+. Thus, in $CaMoO_4$ the ICL from the first discharge and charge should correspond to 2.2 mol of Li, due to $Mo^{6+} \rightarrow Mo^{3.8+}$ formation, in good agreement with our experimental value of 2.1 mol of Li (Figure 7, Table 1, and eqs 1−3). However, the proposed reaction mechanism needs to be confirmed by in situ XRD and physical techniques.

Conclusions

Pure and C-coated $CaMoO_4$ with the scheelite structure in nanocrystalline form were synthesized by room-temperature solution precipitation and sol−gel methods; characterized by X-ray diffraction, SEM, and TEM; and studied as cathode vs Li metal by galvanostatic method and cyclic voltammetry. XRD showed well-defined peaks of the tetragonal structure without any water of hydration for soln ppt $CaMoO_4$. SEM showed that the latter consisted of agglomerates of nanosized particles, whereas

the C-coated $CaMoO_4$ consisted of well-separated and micron-sized particles. Sol−gel $CaMoO_4$ consisted of nanoparticles with size 50−80 nm. TEM confirmed the nanocrystalline nature of $CaMoO_4$ and uniform C-coating, the latter being amorphous. Galvanostatic cycling was carried out over 50 cycles in the range of 0.005−2.5 V at a current rate of 10 mA/g for the first two cycles and at 60 mA/g for all other cycles. Cycling was also performed with upper cutoff voltages of 2.0 and 3.0 V for the sol−gel and C-coated $CaMoO_4$. It was found that the cutoff voltage of 2.5 V gives best performance. At the 20th cycle, the discharge capacities (mA h/g) of $CaMoO_4$ after correcting for carbon content are as follows: soln ppt, 190; sol−gel, 268; 5% C-coated, 401; and 10% C-coated, 508. The C-coating enabled high interparticle electronic conductivity of the otherwise insulating $CaMoO_4$ and resulted in the best performance, with 3.8 mol of recyclable Li (508 mA h/g). The Coulombic efficiency for all the compositions is >98%. The capacity of 5% C-coated $CaMoO_4$ remained stable up to 40 cycles, whereas that of 10% C-coated sample decreased slowly to 439 mA h/g (3.3 mol of Li) in the range of 20−50 cycles. On the other hand, the capacity of sol−gel $CaMoO_4$ increased from 268 to 292 mA h/g during 20−40 cycles and remained stable till the 50th cycle. The CV data compliment the galvanostatic cycling behavior. A plausible mechanism has been proposed for the first discharge and subsequent charge−discharge cycling of $CaMoO_4$. The observed capacities compare well with the graphite negative electrode used in LIB. Further optimization of C-coated $CaMoO_4$ as anode material for LIB is possible, since it is easily synthesized and raw materials are readily available.

Acknowledgment. Thanks are due to Mr. K. W. Ho for help in SEM studies.

CM0348287